

Characterization, Biofilm and Plasmid Curing Effect of Silver Nanoparticles Synthesis by Aqueous Extract of *Myristica fragrans* Seeds

Sabah Mahdi Hadi¹*, Alaa Mohammed Etheb², Afrah Hatem Omran²,
Shamia Hussain Hassan¹

¹University of Baghdad, College of Science, Biology Department, Baghdad, Iraq, ²University of Baghdad, College of Science, Chemistry Department, Baghdad, Iraq

Received: October 28, 2020; Revised: February 6, 2021; Accepted: March 16, 2021

Abstract

Nowadays nanoparticles are used in many fields of life all over the world, and there are numerous ways to obtain them: chemical, physical and biological processes. In recent times, the biological method for the synthesis of nanoparticles associated with using plant extract is widely spread.

Optimal conditions for synthesis of silver nanoparticles using aqueous seeds extract of *Myristica fragrans* were highlighted in this research, such as type of plant extract, weight of extracted plant material, volume ratio of plant extract to AgNO₃ and temperature of reaction.

The study proved that the optimal status for AgNPs synthesis by using 10 g of *M. fragrans* seeds powder were added to 100 mL boiled distilled water, then homogenized and filtered after 24 hours. Aliquot of 5 mL of hot aqueous extract were added to 45 mL of 1*10⁻³ M AgNO₃ solution in the water bath with a magnetic stirrer for the bio-reduction process at 60 °C. The biological activity of AgNPs nanoparticles was evaluated by using well diffusion method and biofilm formation for G+ and G- bacteria including *Escherichia coli*, *Staphylococcus aureus*, *Staphylococcus epidermidis* and *Klebsiella pneumonia*, while the effect of AgNPs nanoparticles on plasmid curing was investigated for *Escherichia coli* and *Staphylococcus aureus* only.

Atomic Force Microscopy (AFM) images proved that Ag particles are in nanometer- size and have granular shape, the size of silver nanoparticle is (74.55 nm) for the sample taken after 16 min of the reaction.

Nanoparticles of various concentrations have proven effective in inhibiting bacterial growth after antimicrobial activity test, biofilm formation and plasmid curing as they exhibited a remarkable effect in inhibiting the growth of both Gram-positive and negative bacteria.

Keywords: silver nanoparticles, green method, biofilm, plasmid curing, *Myristica fragrans*,

1. Introduction

Nanotechnology today is one of the most interesting fields of sciences because of its multifunctional properties, specifically the size range from (1-100) nm (Zia *et al.*, 2016 and Sithara *et al.*, 2017).

The unique size of nanoparticles allowed using them in various fields of applications such as medicine, food, biomedical, electronics, mechanical industries, biotechnology and environmental because of their many properties (Ahmed *et al.*, 2016; Khatoon *et al.*, 2017 and Henríquez *et al.*, 2020). The properties of NPs relay on the specific parameters like shape, size and surface of molecules; while achieved nanoparticles quality is based on their synthesis methods (Kuppusamy *et al.*, 2016 and Sithara *et al.*, 2017).

Song and Kim (2009) reported on the synthesis of Ag nanoparticles by the reduction of Ag⁺ using Pine, Persimmon, Ginkgo, Magnolia and Platanus leaves broth.

The time courses of AgNPs synthesis with different reaction temperatures were studied.

The best reducing agent in the duration of synthesis rate and diversion to silver nanoparticles was Magnolia leaf extract, where the AgNPs was synthesized during 11 min of reaction time and a reaction temperature at 95 °C.

Heydari and Rashidipour (2015) studied the effect of different concentrations of Jaft aqueous extracts (*Quercus infectoria*) on the synthesis of silver nanoparticles; the results showed that increasing the concentration of Jaft aqueous extract led to synthesize more silver nanoparticles.

The classical methods for nanoparticles formation are chemical and physical methods, but they are not eco-friendly because of using many toxic chemical compounds (Carrillo-Lopez *et al.*, 2016 and Kambale *et al.*, 2020). Today, the green method includes the use of plant extracts which is preferable over other methods as they provide reducing agents of secondary metabolites such as flavonoids, alkaloids, phenolics, tannins and terpenoids. Availability of plant sources makes this method easy and

* Corresponding author e-mail: sabahbitech2013@gmail.com.

cost effective (Carrillo-Lopez *et al.*, 2016; Sithara *et al.*, 2017 and Khan *et al.*, 2018).

The Ag nanoparticles are considered as one of the important metallic nanoparticles because of their unique characteristics like catalytic activity, chemical stability and good conductivity, so it is commonly used as anti-bacterial, antifungal, anti-viral and anti-inflammatory (Zhang *et al.*, 2014; Ibrahim, 2015 and Liao *et al.*, 2019). In this study, *Myristica fragrans* seeds called nutmeg belonging to the Myristicaceae family were used for Ag nanoparticles formation.

This aromatic plant has a wide range of active phytochemicals such as alkaloids, terpenoids, phenolic, lignins, tannins, steroids, flavonoids, etc. (Saxena and Patil, 2012; Bindu and Kumar, 2013 and Gupta *et al.*, 2013). The aim of this study is to identify the optimal conditions of AgNPs synthesis such as type of plant extract, temperature, time and the concentration of AgNO₃ to achieve the best concentration of nanoparticles.

2. Materials and Methods

2.1. Preparation of cold, boiling and hot *M. fragrans* aqueous seed extracts

M. fragrans seeds were bought from local market in Baghdad, grinded in electrical grinder for 5-7 min, then 10 g of seeds powder was added to 100 mL of boiling distilled water to prepare hot aqueous extract, while to prepare cold aqueous extract, 10 g of seed powder was soaked in 100 mL distilled water.

A quantity of 10 g of *M. fragrans* seeds powder was added to 100 mL distilled water then heated for 1 hour at 95 °C to prepare the boiling aqueous extract. The three extracts were homogenized by using magnetic stirrer for 3 hours then left overnight at 4 °C. The extracts were filtered using Whatman paper No.1 then centrifuged at 8000 rpm for 10 min and stored at 4 °C until use (Banerjee *et al.*, 2014 and Owaid *et al.*, 2018).

2.2. Preparation of silver nanoparticles using plant extract

AgNPs was synthesized by adding 45 mL of 1*10⁻³ M of AgNO₃ (Sigma-Aldrich) solution in a dark flask placed in a water bath with stirring continuously till the temperature stabilized at 60 °C then 5 mL of seed extract was added (AL-Azawi *et al.*, 2018), 2 mL was taken from the reaction mixture every 2 and 5 min for 20 and 30 min respectively. All samples were measured using UV spectrophotometer; gradually, the change of color to dark brown from light yellow was observed after 2-3 days.

2.3. Characterization of AgNPs

2.3.1. UV spectrophotometer measurement

Preliminary characterization of the AgNPs was carried out using UV-vis spectroscopy. The UV-vis absorption spectra of the AgNPs were measured at room temperature on a spectrophotometer (UV-Spectrophotometer-Shimadzu UV-1800) in 1 cm optical path quartz cuvette. The optical behavior of the biosynthesized AgNPs aliquots of samples were analyzed every 2 min in the range of a wavelength from 190 - 1100 nm (Jain and Mehata 2017).

2.3.2. Fourier Transforms Infrared Spectrophotometer (FTIR) measurement

FTIR measurements were carried out to identify various functional groups in *M. fragrans* extract which are responsible for reducing and stabilizing the synthesized AgNPs. The samples of AgNPs and *M. fragrans* extract were prepared by dropping 3 mL from each sample directly on a glass slide and left to dry at room temperature. The dried samples were grinded with KBr and analyzed on using Shimadzu IR-Affinity¹. (Shanan *et al.*, 2018 and Fatema *et al.*, 2019).

2.3.3. Atomic Force Microscopy (AFM) measurement

The surface morphology of AgNPs was studied by using AFM (Angstrom AA2000, contact mode, atmospheric conditions, USA) images, which clarifying topological images at high magnification of surface morphology. Aliquot of 0.5 mL of AgNPs sample was centrifuged using eppendorf tube for 5 min at 10000 rpm. A few drops from the sample were placed on the slide, air dried and characterized by using atomic force microscopy (Karoutsos, 2009 and Carapeto *et al.*, 2019).

2.4. Identification the optimal conditions for synthesis silver nanoparticles

2.4.1. Evaluation of the optimal temperature in AgNPs synthesis

The optimum temperature for synthesis of AgNPs was determined by added 45 mL of 1*10⁻³ M AgNO₃ solution to 5 mL of hot aqueous extract of *M. fragrans* in a flask placed in a water bath with continuous stirring at different temperatures (40, 50, 60 and 70) °C every time, 2 mL was taken from the reaction mixture every 2 min for 20 min; all samples were measured using UV spectrophotometer immediately and after 15 days (Verma and Mehata, 2016).

2.4.2. Evaluation of the ratio of hot aqueous plant extract to AgNO₃ solution in AgNPs synthesis

Different volumes of hot aqueous plant extracts and AgNO₃ solution were used in synthesis of AgNPs by adding 45, 25 and 5 mL of 1*10⁻³ M AgNO₃ to (5, 25 and 45) mL of hot aqueous plant extract respectively. All the samples were placed in a water bath at 60 °C with continuous stirring then measured using UV spectrophotometer (Ibrahim, 2015 and Ahmed *et al.*, 2016).

2.4.3. The effect of difference in plant material weight on the preparation of *M. fragrans* hot aqueous extract in AgNPs synthesis

The hot aqueous extracts of *M. fragrans* were prepared using different weights of seeds powder (6, 8 and 10) g then extracted in 100 mL of boiling distilled water. AgNPs was synthesized by adding 45 mL of AgNO₃ solution to 5 mL of plant extract every time of reaction as mentioned above; 2 mL was taken from the reaction mixture every 5 min for 20 min then all samples were measured using UV spectrophotometer (Sithara *et al.*, 2017).

2.5. Biological activity

2.5.1. Antimicrobial activity

The antimicrobial activity of silver nanoparticles was investigated using the well diffusion method on Mueller-Hinton agar (MHA) (Merck). The inhibition zones were

reported in millimeter (well size was 6 mm) against various sorts of bacteria like gram negative bacteria (*Escherichia coli*, *Klebsiella pneumoniae*) and gram positive bacteria (*Staphylococcus aureus*, *Staphylococcus epidermidis*).

MHA agar plates were inoculated with bacterial strain under aseptic conditions and wells were filled with 50 μL at various concentrations of AgNPs (100, 75, 50 and 25) % and incubated at 37 °C for 24 hours. After the incubation period, the inhibition zones were measured (Ibrahim, 2015).

2.5.2. Determination of minimum inhibitory concentration (MIC)

AgNPs was used to determine MIC for planktonic cells of *E. coli*, *K. pneumoniae*, *S. aureus* and *S. epidermidis* bacteria. MIC test was conducted in 96- well microtiter plate; each test well was filled with 100 μL Trypton soya broth (TSB) (Merck) + 1% w/v glucose (BHD). Aliquot of 100 μL of AgNPs was added to the first test well then mixed well to prepare a double series of dilutions across the plate.

Aliquot of 10 μL of bacterial suspension was placed in each well plate to achieve a final inoculum size of 4×10^5 CFU / mL. The positive control was achieved by adding TSB and bacterial inoculum without adding AgNPs to the well. Negative control was achieved by adding AgNPs without inoculum. After incubation for 18- 24 h at 37 °C, the microbial growth in the well was examined by turbidity. The MIC value was described as the lowest AgNPs concentration inhibits 80% of microbial growth, relative to the negative and positive controls (Christensen *et al.*, 1995).

2.5.3. Biofilm activity

Biofilm formation test was achieved by using 96- well microtiter plate (Sánchez *et al.*, 2016). *E. coli*, *K. pneumoniae*, *S. aureus* and *S. epidermidis* bacteria were cultured in Trypton soya (TS) broth for 24 h then the resulting culture was diluted to 1:100 TSB (Merck) + 1% w/v glucose (BHD). Each well of microplate was loaded with 100 μL of TSB and 100 μL of AgNPs produced from 12 and 16 min except the control well without AgNPs, then microplate, was incubated at 37 °C for 24 h, and each concentration was carried out in triplicate.

The planktonic bacteria were removed by washing the microtiter plate with sterile distilled water for 3 times; subsequently, 0.1% w/v crystal violet solution was added to each well then left to stain for 10 min at 25 °C. The crystal violet dye was removed by immersing the plate in a water tray, then inverting on paper towels to remove excess liquid and left to air dry. The plate was treated with ethanol 96% for 10-15 min at 25 °C to solubilize the dye bound, and then absorbance was measured at 630 nm (AL-Azawi *et al.*, 2019).

2.5.4. Plasmid curing

The bacterial DNA plasmid was extracted by using alkaline lysis method. The pathogenic bacteria *E. coli* and *S. aureus* were inoculated into 5 mL Nutrient broth (Merck) tubes after being treated with different concentrations (0.5, 1, 3 and 6) % of silver nanoparticles of the samples 12 and 16. All the tubes were incubated for 24 hours at 37 °C with shaking except the control tubes (without AgNPs). The extraction of plasmid DNA was

carried out according to the Green and Sambrook, (2012) method.

3. Results and Discussion

Differences in physical and chemical conditions such as type of extraction, temperature, reaction period, weight of plant material and reactants concentration significantly affected the form, size and the morphology of Ag nanoparticles.

2.6. Visual observation of AgNPs

At the beginning of the reaction between *M. fragrance* extract and AgNO_3 solution, the reaction mixture was transparent, but over time the solution changed to light yellow and then to light brown. The chromatic change in the solution indicates the formation of AgNPs (Pirtarighat *et al.*, 2019). After about two weeks, the color of the solution turns dark brown with increasing color intensity as shown in Figure 1.

Increasing incubation time of the solution enhanced the growth of silver nanoparticle, and this result corresponds with the result of Ibrahim, 2015. Also, the presence of secondary metabolites in the plant extracts such as alkaloids and flavonoids that provide the electronic capacity of reduction Ag^+ to Ag^0 as mentioned by Sharma *et al.*, 2014; Verma and Mehata, 2016; Izah *et al.*, 2018 and Khan *et al.*, 2018.

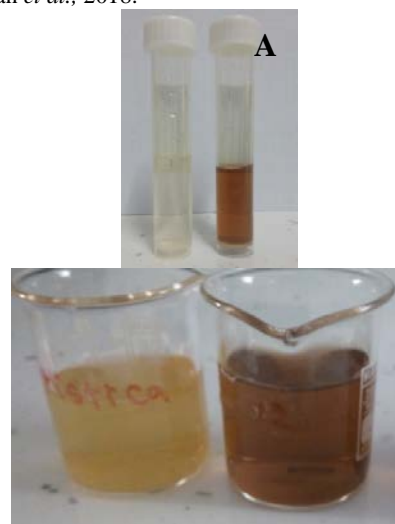


Figure1. The change in color of AgNPs solution over time after adding *M. fragrance* seeds extract to 10^{-3}M AgNO_3 (A) Left: 10^{-3}M aqueous silver nitrate. Right: AgNO_3 with *M. fragrance* seed extract forming AgNPs after two weeks. (B) Left: *M. fragrance* seeds aqueous extract 100 g/L. Right: 10^{-3}M AgNO_3 with the seed extract forming AgNPs after two months.

2.7. Characterization of AgNPs biosynthesis and the effect of reaction time on the formation of silver nanoparticles

2.7.1. UV-vis spectrophotometric analysis was carried out as first identify for AgNP formation.

Different components may contribute to the reduction of Ag ions during AgNPs biosynthesis by using plant extract. Figure 2 shows the visible spectrum of ultraviolet radiation for AgNPs obtained from the reaction of *M. fragrance* hot extract and 10^{-3} M AgNO₃ recorded 200 to 800 nm at regular intervals every two minutes. The maximum absorption observed and represented the extreme energy is 416 nm as obtained by Sharma *et al.*, 2014 and Ibrahim, 2015 showing that the synthesized of AgNPs are smaller with steady size distribution. It is noted from Figure 2 the absorption spectra due to the rapprochement of reaction time.

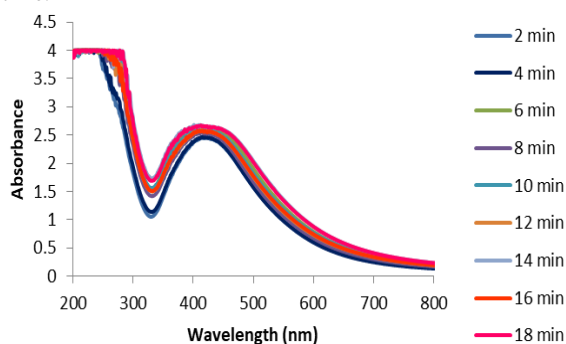


Figure 2. Absorption spectra of silver nanoparticules at various reaction time intervals of 10^{-3} M AgNO₃ with *M. fragrance* seed extract.

Time represents an important factor in the formation of silver nanoparticles. Figure 3 represents the absorption spectra of silver nanoparticles at 60 °C and at various reaction time intervals, every 5 min which was measured after 7 days of reaction. No visible peaks were observed.

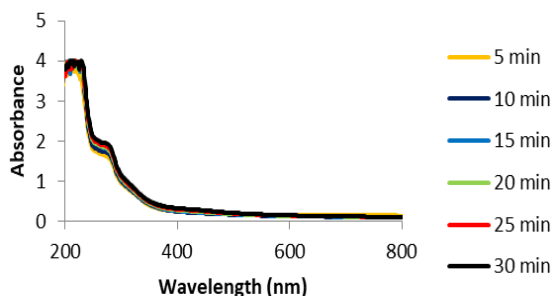


Figure 3. Absorption spectra of AgNPs at various reaction time intervals of *M. fragrance* hot aqueous extract and 10^{-3} M AgNO₃ at 60 °C after 7 days of reaction.

Ten days after the reaction, we observe the appearance of absorption spectra of nanoparticles and for all reaction times. The UV-vis data in Figure 4 shows a distinct peak at 416 nm is observed at all times of reaction (5-30) min. The figure also shows that the peaks at all times are identical with each other and similar to the absorption spectra in Figure 1. This indicates the formation of silver nanoparticles at all reaction times, and this is consistent with the results of Song and Kim, 2009; Verma and Mehata, 2016 and Sithara *et al.*, 2017.

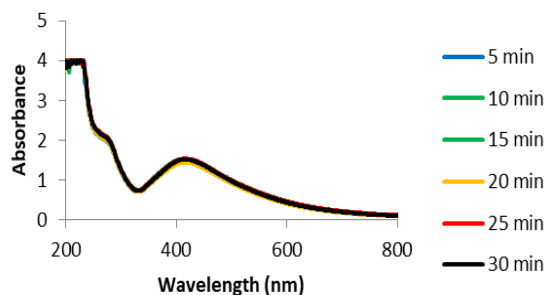


Figure 4. Absorption spectra of AgNPs at various reaction time intervals of *M. fragrance* hot aqueous extract and 10^{-3} M AgNO₃ at 60 °C after 15 days of reaction.

From the UV-VIS analysis, in Figure 5 that showed an increase in the absorbance with time indicating an increase in the forming of AgNPs a broad-spectrum bell-shaped curve was obtained in the range 350-550 nm. A Distinct peak at 416 nm showed a sharp surface plasmon resonance (SPR), which was specified for silver nanoparticles (Mahendran and Kumari, 2016; Owaied *et al.*, 2018 and Pirtarighat *et al.*, 2019).

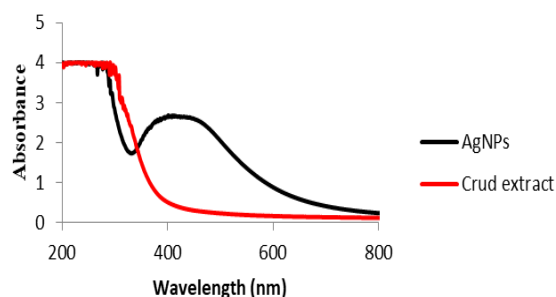


Figure 5 . Absorption spectra of silver nanoparticules and *M. fragrance* hot aqueous extract.

The effect of using different plant extraction methods in AgNPs synthesis

The results in figure 6 show increasing synthesis rate of AgNPs by using the hot aqueous extract of *M. fragrance*, then the boiling and cold plant extract. The extraction method may be the reason for this behavior which is due to the ionization of secondary compounds existing in aqueous extract and responsible for the reduction of silver salt to silver ions as a reducing agent, specially the essential oil and phenolic compounds found in nutmeg in large quantities (Raphael *et al.*, 2010; Enabulele *et al.*, 2014).

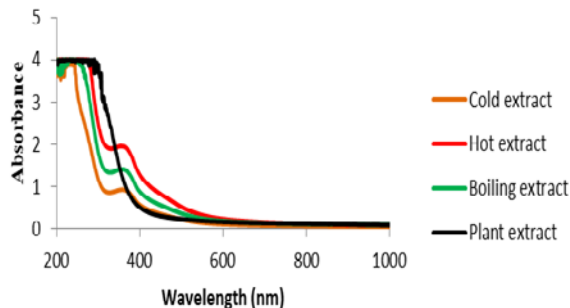


Figure 6 . Absorption spectra of AgNPs obtained from different aqueous extract methods for *M. fragrance* seeds with 10^{-3} M AgNO₃.

It is observed (Figure 6) that nanoparticles are formed clearly by using the three different aqueous extracts of *M. fragrance* seeds after interaction with silver salt (Sharma *et al.*, 2014; Verma and Mehata, 2016).

The effect of using different temperatures on AgNPs synthesis

The reaction mixture was exposed to different temperatures varying from 40 °C to 70 °C. The varying temperatures with the variation in absorbance of AgNPs synthesis were observed (Figure 7) indicating that temperature has altered the rate of AgNPs reaction. The highest rate of spectra value was at 60 °C then 40 °C but the lowest rate of spectra was at 50 °C and 70 °C.

The optimum temperature for AgNPs formation was recorded at 60 °C, indicating that small Ag nanoparticles are formed at this temperature (Zia *et al.*, 2016). As the temperature of reaction increased, both the rate of synthesis and the final conversion of silver nanoparticles increased (Song and Kim, 2009 and Ibrahim, 2015).

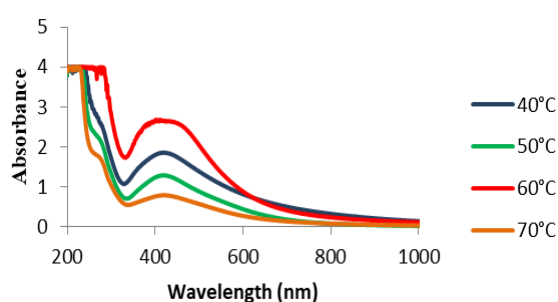


Figure 7. Absorption spectra of AgNPs prepared at different reaction temperatures of 40, 50, 60 and 70 °C.

The effect of using different plant weights on AgNPs synthesis

For complete reduction of Ag ions to silver nanoparticles, three different weights of *M. fragrance* seeds were used to prepare the hot aqueous extract then mixed separately with a fixed volume of 10^{-3} M AgNO₃. The outcome in Figure 8 shows that at high concentration of 10 g / 100 mL of hot extract led to synthesizing more silver nanoparticles better than 6 and 8 g / 100 mL (Heydari and Rashidipour, 2015), which indicates there is a direct interconnection between the extract concentration and the synthesis of silver nanoparticles.

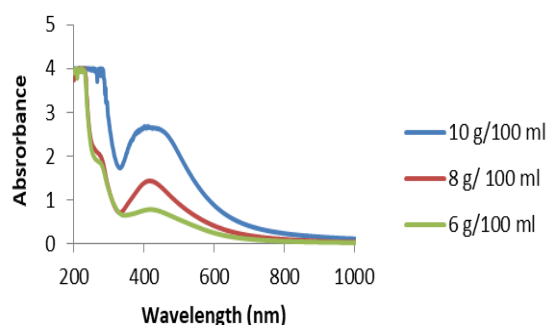


Figure 8. Absorption spectra of AgNPs at different weights of *M. fragrance* seeds extracts and 10^{-3} M AgNO₃.

The increase in extract concentration leads to rising in the rate of secondary compounds and thus increasing the reduction of silver salt to silver ions.

The effect of using different volumes of aqueous hot broth on AgNPs synthesis

Another important variable that determines the optimal volume of the extract reacts with silver salt to produce nanoparticles. Figure 9 shows the UV-visible spectra of nanoparticles obtained from the reaction of three different quantities of *M. fragrance* seeds hot extract and 10^{-3} M AgNO₃.

When increasing the volume of seed extract to silver nitrate to the ratio 45:5, 25:25 mL, no absorption band was observed. While decreasing the volume in the reaction mixture to 5:45 mL, the absorption was observed at 416 nm, indicating the enhancement in the synthesis of silver nanoparticles (Heydari and Rashidipour, 2015).

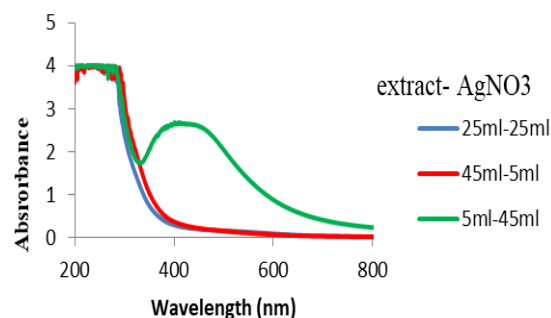


Figure 9. Absorption spectra of AgNPs at various volumes of *M. fragrance* hot aqueous extracts and 10^{-3} M AgNO₃ (25:25, 45:5, 5:45) mL.

2.7.2. FTIR spectroscopy analysis

FTIR measurement was carried out to identify various functional groups in *M. fragrans* seed extract and predicting their role in the synthesis of Ag NPs. The FTIR spectra of nutmeg extract and AgNPs is shown in Figure 10 (a), (b) and (c) showing strong and broad range peak at 3441 cm^{-1} , that assigned for OH stretching in alcohols and phenolic compounds (Sharma *et al.*, 2014 and Sivaprakash *et al.*, 2019).

Shifting to the lower frequency 3442 cm^{-1} and 3439 cm^{-1} for silver nanoparticles at 12 and 16 min respectively may indicate the involvement of the O-H functional group in the synthesis of nanoparticles. The absorption peak at 1627 cm^{-1} could be assigned to the $\nu\text{ C=N}$ stretching in the amide group in the seeds extract. The shift in this peak from 1627 cm^{-1} to 1635 cm^{-1} and 1637 cm^{-1} of AgNPs that synthesized at 12 and 16 min respectively indicates the possible involvement of amide group in *M. fragrans* seed extract in nanoparticle synthesis.

The peak at 1066 cm^{-1} may attributed to the C-O group in crude seeds extract which shifted to 1062 cm^{-1} and 1060 cm^{-1} in silver nanoparticles at 12 and 16 min respectively after the reduction of silver. The FTIR results displayed that the biological molecules performed dual functions of synthesis and stabilization of AgNPs in the aqueous broth (Erjaee *et al.*, 2017; Khan *et al.*, 2018).

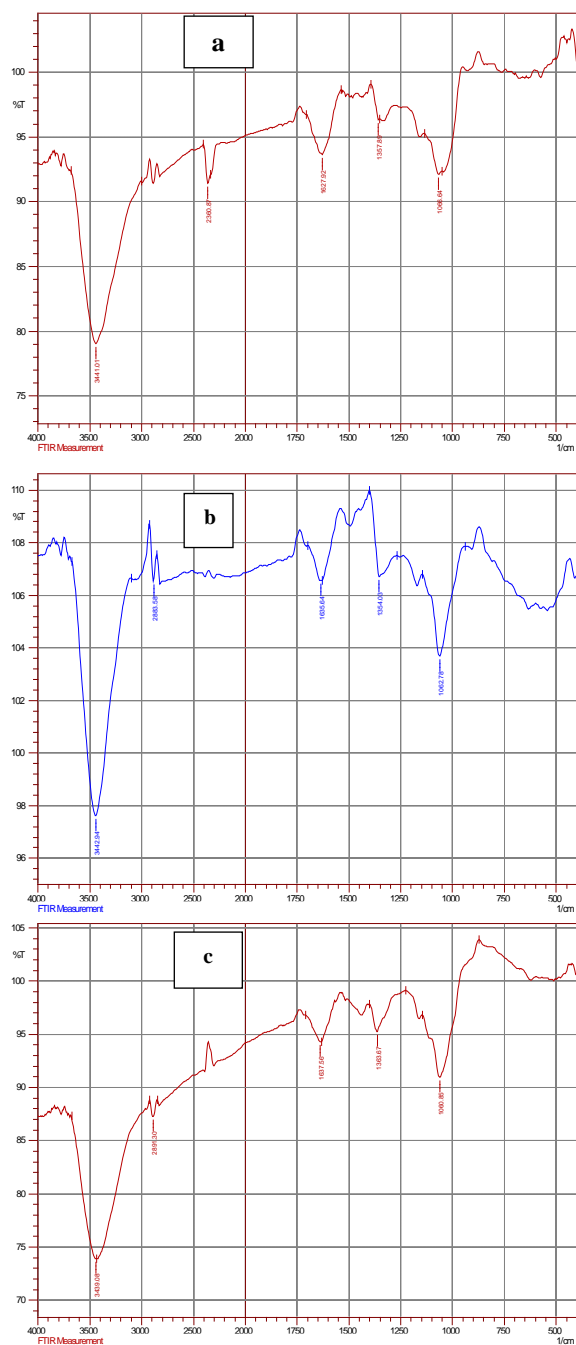


Figure 10. FTIR spectra of (a) *M. fragrans* aqueous extract (b) AgNPs in 12 min (c) AgNPs in 16 min.

2.7.3. Atomic Force Microscopy (AFM) analysis

AFM analysis is used to study the surface morphology of nanoparticles (Shkryl *et al.*, 2018). AFM images can determine the size, conglomerate, and surface roughness of silver nanoparticles (Majeed *et al.*, 2015 and Fatema *et al.*, 2019). The circumstances of an experiment are highly influence nanoparticles distribution and differences in size, and capability for aggregation.

Many shapes of ANPs appeared after synthesis by using the green method, like spheres, plates, rods and needles. The form of silver nanoparticles depends on the kind of plant and the concentration of plant broth, the rate of adding the plant extract and silver salt to the reaction, time of reaction, temperature, pH, etc. (Fatema *et al.*, 2019).

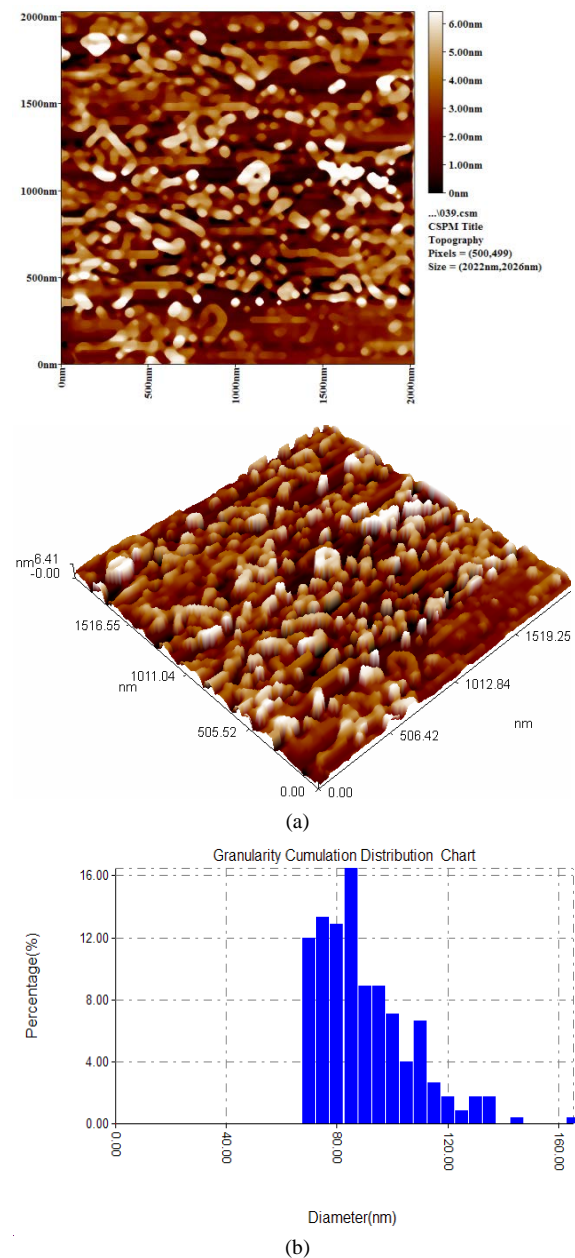


Figure 11. AFM topography for Ag nanoparticles (a) 2D & 3D AFM images of AgNPs that synthesized at 60 °C after 12 min of reaction. (b) Granularity distribution of AgNPs that synthesized at 60 °C after 12 min of reaction.

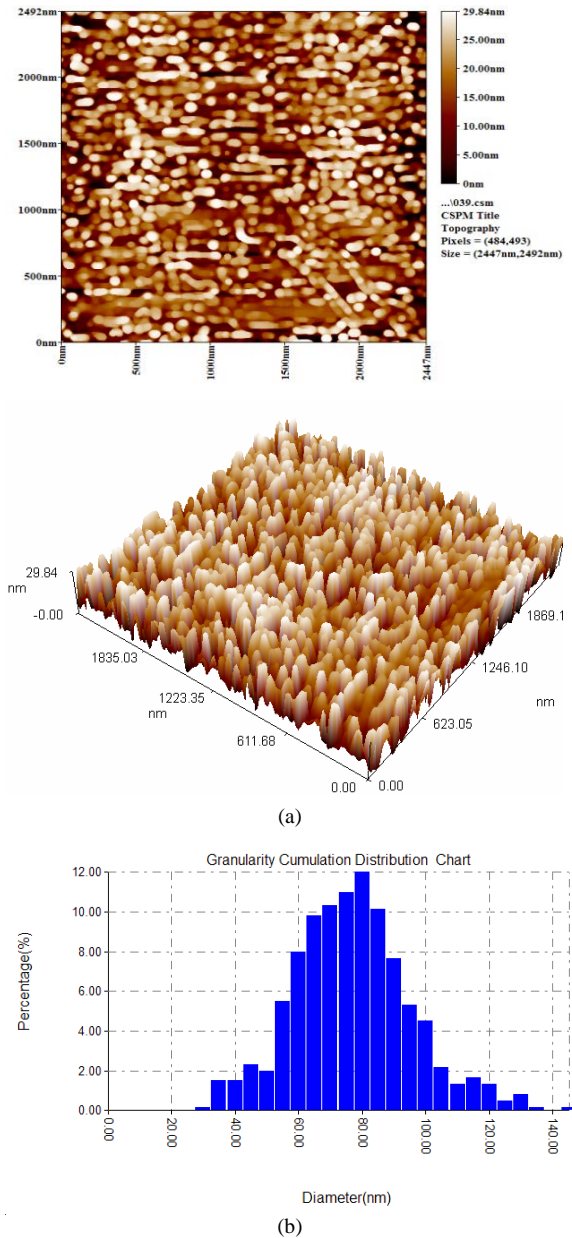


Figure 12. AFM topography for Ag nanoparticles (a) 2D & 3D AFM images of AgNPs that synthesized at 60 °C after 16 min of reaction. (b) Granularity distribution of AgNPs that synthesized at 60 °C after 16 min of reaction.

AFM images in Figure 11 (a) and 12 (a) show that Ag particles are in nanometer- size and granular shape. The size of silver nanoparticles were 87.71 nm and 74.55 nm for the samples taken after 12 min and 16 min of reaction as shown in Figure 11 (b) and 12 (b) respectively. The grain size rate decreasing with increasing the reaction time by increasing the silver salt reduction due to the ionization of secondary compounds as stated by AL-Azawi *et al.*, (2018).

2.8. The biological activity results

2.8.1. Antimicrobial activity of Ag NPs samples

Antibacterial activity of AgNPs samples a (12) and b (16) was studied against gram negative bacteria (*Escherichia coli*, *Klebsiella pneumoniae*) and gram positive bacteria (*Staphylococcus aureus*, *Staphylococcus epidermidis*). The results show that the size of the

nanoparticles and the kinds of bacteria under consideration have a great effect on the inhibition zone size. Figure 13 a shows that AgNPs sample (12) at the concentrations 100, 75, 50 and 25% caused the highest inhibition effect against *S. epidermidis* bacteria, and these results are compatible with the results of Netala, *et al.*, (2014) while the lowest inhibition effect for silver nanoparticles in all concentrations was against *S. aureus*. Both *E. coli* and *K. pneumoniae* bacteria achieved almost the same inhibition zone against using the nanoparticles in all its concentrations. Figure 13 b displays AgNPs sample 16 at 100% concentration exhibiting the highest inhibition effect against *E. coli* bacteria, and this is consistent with the results of Paul and Sinha, (2014). While *S. epidermidis* bacteria showed the highest inhibition zone when treated with silver nanoparticles at the concentrations 75, 50, and 25%, then *E. coli* bacteria at the same concentrations. While *K. pneumoniae* and *S. aureus* resulted in the same inhibition effect when tested in the presence of AgNPs sample 16 in all the concentrations.

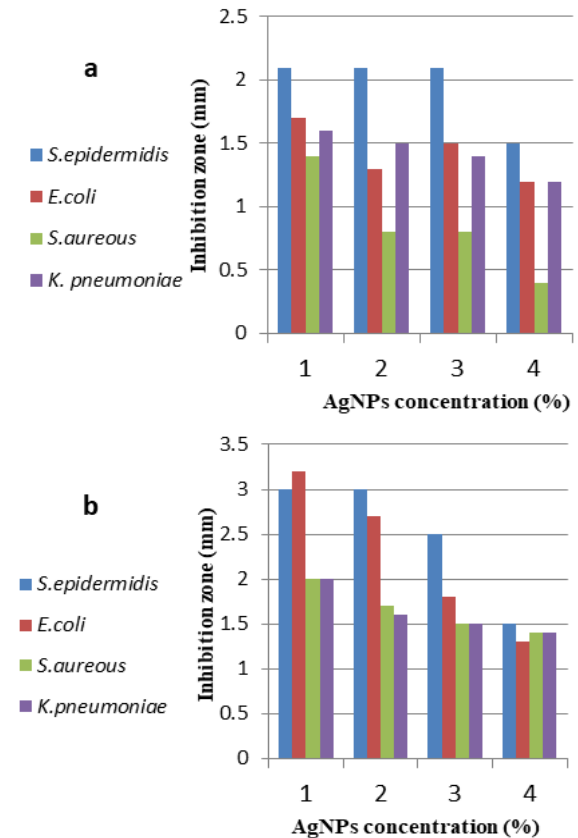


Figure 13. The effect of Ag NPs samples a (12) and b (16) on biological activity of pathogenic bacteria by using different concentrations (1) 100%, (2) 75%, (3) 50%, (4) 25% from silver nanoparticles.

2.8.2. Estimation of AgNPs effect on the biofilm formation inhibition by pathogenic bacteria

The influence of Ag nanoparticles on biofilm formation inhibition was clear for gram negative and positive pathogenic bacteria. The results confirm that there was an inverse relationship between the concentration of nanomaterials and the inhibitory effect of biofilm formation.

The lower the silver concentration, the more inhibiting effect on bacteria biofilm formation. The results also

proved that the lowest size of Ag nanoparticles sample (b) 16 (74.55) nm had a better inhibition effect on all bacterial strains than Ag nanoparticles sample (a) 12 (87.71) nm. It was observed that the highest effect of the biofilm inhibition for both nanoparticle samples 12 and 16 belonged to *K. pneumoniae* as shown in Figure 14.

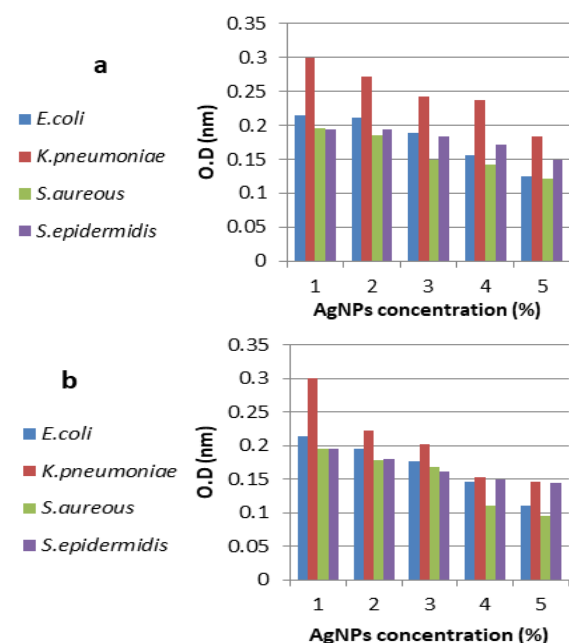


Figure 14. The effect of AgNPs samples a (12) and b (16) on inhibition of biofilm formation by pathogenic bacteria using different concentrations (1) (control) normal growth of pathogenic bacteria without AgNPs (2) 100%, (3) 75%, (4) 50%, (5) 25% from silver nanoparticles.

Both *E. coli* and *S. aureus* exhibited a convergent inhibition effect, while *S. epidermidis* bacteria showed the lowest inhibition effect compared with the control. AgNPs at the concentration 25% achieved the highest inhibition effect to biofilm formation among all the pathogenic bacteria, while the concentration 100% showed the lowest inhibition effect to biofilm formation among all pathogenic bacteria.

The best inhibiting biofilm effect of *K. pneumoniae* bacteria by using AgNPs was at the concentrations 25, 50, 75 and 100% respectively compared with the control while *S. epidermidis* showed less inhibition effect to biofilm formation at all the concentrations of AgNPs. The effect of AgNPs on Gram negative bacteria was better than the effect on Gram-positive bacteria. The mechanism of AgNPs activity occurs due to the correlation of AgNPs to the bacteria cell wall and then generating the free radicals (Pirtarighat *et al.*, 2019). Silver nanoparticles bind to the cell membrane, forming pores that increase membrane permeability and cause cell death (Netala *et al.*, 2014; Verma and Mehata, 2016 and Pirtarighat *et al.*, 2019).

2.8.3. Estimation the effect of AgNPs on plasmid curing of pathogenic bacteria

The AgNPs samples (12 and 16) displayed a clear inhibition effect on both Gram positive and negative bacteria as antiplasmid DNA activity shown in Figure 15.

S. aureus bacteria exhibited the highest inhibition effect for the entire concentrations (0.5, 1, 3 and 6) % for both samples 12 and 16 of silver nanoparticles compared with the control. *E. coli* bacteria followed the same behavior

after being treated with the AgNPs samples 12 and 16 in all concentrations except 0.5% from sample 12 which displayed less effect as anti plasmid.

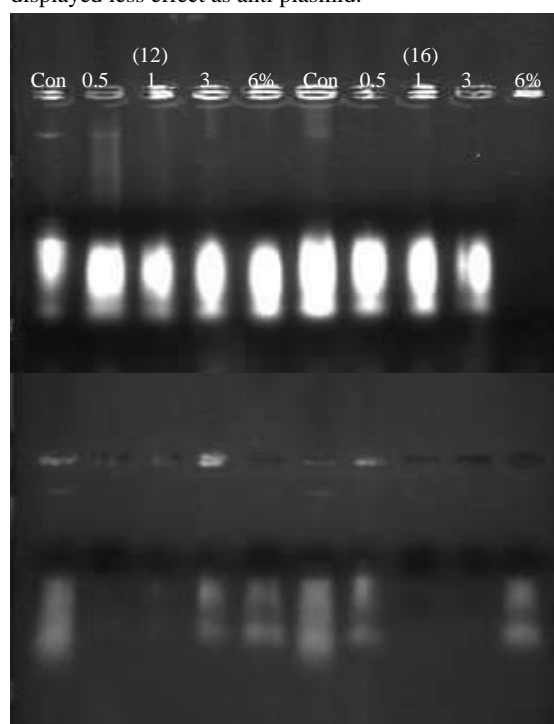


Figure 15. Agarose gel electrophoresis profile of plasmid DNA for *E. coli* and *S. aureus* bacteria after being treated with different concentrations (0.5, 1, 3 and 6) % from 12 and 16 samples of AgNPs, left: *E. coli* bacteria, right: *S. aureus* bacteria.

The results also proved that the lowest size of Ag nanoparticles sample (b) 16 (74.55) nm caused a better inhibitory effect as antiplasmid on pathogenic bacteria strains than Ag nanoparticles sample (a) 12 (87.71) nm.

3. Conclusion

The green synthesis of nanoparticles by using a green reduction agent is an ecofriendly, cheap, and effective method. In this study, AgNPs nanoparticles were synthesized by using the hot aqueous extract of *M. fragrance*. The chromatic change in the solution confirmed the formation of silver nanoparticles.

UV-vis spectra displayed a special peak for silver at 416 nm which was conformable to the surface plasmon peak of Ag nanoparticles; in addition, formation of silver nanoparticles occurred at all reaction times. The use of hot aqueous extract of *M. fragrance* increased the synthesis rate of Ag nanoparticles, especially after using 10 g / 100 mL from plant seeds to prepare the hot aqueous extract. The convenient temperature for AgNPs formation was

60 °C, which indicates that a small Ag nanoparticle was formed at this temperature. While the optimal volume of the extract that reacts with silver salt to produce nanoparticles was 5:45 ml.

The FTIR results showed that the biological molecules are forming dual functions of synthesis and stabilization of AgNPs in the aqueous broth. AFM images prove that Ag particles were nanometer-size and had a granular shape.

The grain size rate decreased with increasing the time of reaction, the size of silver nanoparticle was 74.55 nm for the sample taken after 16 min of the reaction. The Ag

nanoparticles in the samples 12 and 16 in all concentrations showed the highest inhibition effect as antibacterial against *S. epidermidis* bacteria.

The influence of Ag nanoparticles on biofilm formation inhibition showed that the lowest size of AgNPs sample 16 (74.55) nm caused a better inhibition effect on all bacterial strains, while the highest effect of the biofilm inhibition for both nanoparticle samples 12 and 16 belonged to *K. pneumoniae*. The results proved that the lowest size of Ag nanoparticles sample (b) 16 (74.55) nm had a better inhibitory effect as anti plasmid on *S. aureus* bacteria strains than Ag nanoparticles sample (a) 12 (87.71) nm.

Acknowledgement

The authors acknowledge the Postgraduate Laboratory staff, Department of Biology, and College of Science at the University of Baghdad.

References

- Ahmed S, Ahmad M, Swami BL and Ikram S. 2016. A review on plants extract mediated synthesis of silver nanoparticles for antibacterial application: A green expertise. *J Adv Res.*, **7**: 17-28.
- AL-Azawi MT, Hadi SM and Mohammed CH. 2018. Ag-SiO₂ nanoparticles prepared by Sol-Gel methods for antibacterial effect. *Iraqi J Physics.*, **16**: 135-151.
- AL-Azawi MT, Hadi SM and Mohammed CH. 2019. Synthesis of silica nanoparticles via green approach by using hot aqueous extract of thuja orientalis leaf and their effect on biofilm formation. *Iraqi J Agric Sci.*, **50**:245-255.
- Banerjee P, Satapathy M, Mukhopahayay A and Das P. 2014. Leaf extract mediated green synthesis of silver nanoparticles from widely available Indian plants: synthesis, characterization, antimicrobial property and toxicity analysis. *Bioresources Bioprocessing.*, **1**: 1-10.
- Bindu NHS and Kumar SR. 2013. In-Vitro assimilation of trimyristin in the seeds of *Myristica fragrans* and in poly herbal ayurvedic formulation by uflc method. *Asian J Pharm Clin Res.*, **6**: 140-145.
- Carapeto AP, Ferraria AM and Botelho AM. 2019. Silver nanoparticles on cellulose surfaces: quantitative measurements. *Nanomaterials.*, **9**:780-788.
- Carrillo-López LM, Soto-Hernández RM, Zavaleta-Mancera HA and Vilchis-Néstor AR. 2016. Study of the performance of the organic extracts of chenopodium ambrosioides for Ag nanoparticle synthesis. *J Nanomater.*, **2016**: 1-13.
- Christensen GD, Simpson WA and Younger JA. 1995. Adherence of coagulase negative Staphylococci to plastic tissue cultures: a quantitative model for the adherence of Staphylococci to medical devices. *Clin Microbiol.*, **22**: 996-1006.
- Enabulele SA, Oboh FOJ and Uwadiae EO. 2014. Antimicrobial, nutritional and phytochemical properties of *Monodora Myristica* seeds. *IOSR J Pharm Biol Sci.*, **9**: 01-06.
- Erjaee H, Rajaian H and Nazifi S. 2017. Synthesis and characterization of novel silver nanoparticles using Chamaemelum nobile extract for antibacterial application. *Adv Nat Sci: Nanosci Nanotech.*, **8**:1-9.
- Fatema S, Shirsat M, Farooqui M and Arif PM. 2019. Biosynthesis of silver nanoparticle using aqueous extract of *Saraca asoca* leaves, its characterization and antimicrobial activity. *Int J Nano Dimens.*, **10**:163-168.
- Green MR and Sambrook J. 2012. **Molecular Cloning**, fourth ed. Cold Spring Harbor, New York.
- Gupta AD, Bansal VK, Babu V and Maithil N. 2013. Chemistry, antioxidant and antimicrobial potential of nutmeg (*Myristica fragrans* Houtt). *J Genet Eng Biotech.*, **11**: 25-31.
- Henríquez LC, Aguilar KA, Álvarez JU, Fernández LV, Oca-Vásquez GM and Baudrit JR. 2020. Green synthesis of gold and silver nanoparticles from plant extracts and their possible applications as antimicrobial agents in the agricultural area. *Nanomaterials.*, **1763**: 2-24.
- Heydaril R and Rashidipour M. 2015. Green synthesis of silver nanoparticles using extract of oak fruit hull (Jaft): synthesis and in vitro cytotoxic effect on MCF-7 cells. *Int J Breast Cancer.*, **2015**: 1-6.
- Ibrahim HM. 2015. Green synthesis and characterization of silver nanoparticles using banana peel extract and their antibacterial activity against representative microorganisms. *J Radiat Res App Sci.*, **8**: 265-275.
- Izah SC, Zige DV, Alagoa KJ, Uhunmwangho EJ and Iyamu AO. 2018. *EC Pharmacol Toxicol.*, **64**: 291-295.
- Jain S and Mehata MS. 2017. Medicinal plant leaf extract and pure flavonoid mediated green synthesis of silver nanoparticles and their enhanced antibacterial property. *Sci Rep.*, **7**: 1-13.
- Kambale EK, Nkanga CI, Mutonkole BI, Bapolisi AM, Tassa DO, Liesse JI, Krause RWM and Memvanga PB. 2020. Green synthesis of antimicrobial silver nanoparticles using aqueous leaf extracts from three Congolese plant species (*Brillantaisia patula*, *Crossopteryx febrifuga* and *Senna siamea*). *Heliyon.*, **4493**: 1-9.
- Karoutsos V. 2009. Scanning probe microscopy: instrumentation and applications on thin films and magnetic multilayers. *J Nanosci Nanotech.*, **9**: 6783-6798.
- Khan MZH, Tareq K, Hossen MA and Roki MN. 2018. Green synthesis and characterization of silver nanoparticles using *Coriandrum sativum* leaf extract. *J Eng Sci Tech.*, **13(1)**: 158 – 166.
- Khan SU, Saleh TA, Wahab A, Khan MHU, Khan D, Khan WU, Rahim A, Kamal S, Khan FU and Fahad S. 2018. Nanosilver: new ageless and versatile biomedical therapeutic scaffold. *Int J Nanomed.*, **13**: 733-762.
- Khatoun N, Mazumder JH and Sardar M. 2017. Biotechnological applications of green synthesized silver nanoparticles. *J Nanosci Curr Res.*, **2**: 1-6.
- Kuppusamy P, Yusoff MM, Maniam GP and Govindan N. 2016. Biosynthesis of metallic nanoparticles using plant derivatives and their new avenues in pharmacological applications – an updated report. *Saudi Pharm J.*, **24**: 473-484.
- Liao C, Li Y and Tjong SC. 2019. Bactericidal and cytotoxic properties of silver nanoparticles. *Int j Mol Sci.*, **20**: 449-496.
- Mahendran G and Kumari BDR. 2016. Biological activities of silver nanoparticles from *Nothapodytes nimmoniana* (Graham) Mabb. Fruit extracts. *Food Sci Human Wellness.*, **5**: 207-218.
- Majeed S, Abdullah MS, Dash GK and Nanda A. 2015. Facile and green synthesis of silver nanoparticles from *Penicillium italicum* and its antimicrobial property in combination with Sparfloxacin. *J Chem Pharma Res.*, **7**: 27-33.
- Netala VR, Kotakadi VS, Nagam V, Bobbu P, Ghosh SB and Tarte V. 2014. First report of biomimetic synthesis of silver nanoparticles using aqueous callus extract of *Centella asiatica* and their antimicrobial activity. *Appl Nanosci.*, DOI 10.1007/s13204-014-0374-6.
- Owaid MN, Muslim RF and Hamad HA. 2018. Mycosynthesis of silver nanoparticles using *Terminia sp.* desert truffle, pezizaceae, and their antibacterial activity. *Jordan J Bio Sci.*, **11(4)**: 401-405.

- Paul D and Sinha SN. 2014. Extracellular synthesis of silver Nanoparticles using *Pseudomonas aeruginosa* KUPSB12 and its antibacterial activity. *Jordan J Bio Sci.*, **7**:245-250.
- Pirtarighat S, Ghannadnia M and Baghshahi S. 2019. Green synthesis of silver nanoparticles using the plant extract of *Salvia spinosa* grown in vitro and their antibacterial activity assessment. *J Nan Chem.*, **9**: 1-9.
- Raphael EC, Gideon OL and Perpetua NU. 2010. Biochemical characteristics of the african nutmeg *Mondora myrsiyica*. *Agric J.*, **5**: 303-308.
- Sánchez E, Morales CR, Castillo S, Rivas CL, Becerra LG and Martínez DMO. 2016. Antibacterial and antibiofilm activity of methanolic plant extracts against nosocomial microorganisms. *Evidence-Based Complement and Alternat Med.*, **2016**: 1-8.
- Saxena, R. and Patil, P., 2012. Phytochemical studies on *Myristica fragranca* essential oil. *Biological Forum – An Int J.*, **4**: 62-64.
- Shanan ZJ, Hadi SM and Shanshool SK., 2018. Structural analysis of chemical and green synthesis of CuO nanoparticles and their effect on biofilm formation. *Baghdad Sci J.*, **15**:211-216.
- Sharma G, Sharma AR, Kurian M, Bhavesh R, Nam JS and Lee SS. 2014. Green synthesis of silver nanoparticle using *Myristica fragrans* (nutmeg) seed extract and its biological activity. *Digest J Nan Biostructures.*, **9**: 325-332.
- Shkryl YN, Veremeichik GN, Kamenev DG, Gorpenchenko TY, Yugay YA, Mashtalyar DV, Nepomnyaschiy AV, Avramenko TV, Karabtsov AA, Ivanov VV, Bulgakov VP, Gnedenkov SV, Kulchin YN and Zhuravlev YN. 2018. Green synthesis of silver nanoparticles using transgenic *Nicotiana tabacum* callus culture expressing silicatein gene from marine sponge *Latrunculia oparinae*. *Artificial Cells, Nanomed Biotech.*, **46**: 1646–1658.
- Sithara R, Selvakumar P, Arun C, Anandan S and Sivashanmugam P. 2017. Economical synthesis of silver nanoparticles using leaf extract of *Acalypha hispida* and its application in the detection of Mn(II) ions. *J Adv Res.*, **8**: 561-568.
- Sivaprakash G, Mohanrasu K, Ravindran B, Chung WJ, AL Farraj DA, Elshikh DS, AL Khulaifi MM, ALKufeidy RM and Arun A. 2019. Integrated approach: Al₂O₃-CaO Nanocatalytic biodiesel production and antibacterial potential silver nanoparticle synthesis from *Pedaliium murex* extract. *J of King Saud University – Sci.*, <https://doi.org/10.1016/j.jksus.2019.12.004>.
- Song JY and Kim BS. 2009. Rapid biological synthesis of silver nanoparticles using plant leaf extracts. *Bioprocess Biosyst Eng.*, **32**:79–84.
- Verma A and Mehata MS. 2016. Controllable synthesis of silver nanoparticles using Neem leaves and its microbial activity. *J Rad Res App Sci.*, **9**: 109-115.
- Zhang C, Liang Z and Hu Z. 2014. Bacterial response to a continuous long-term of silver nanoparticles at sub-ppm silver concentrations in a membrane bioreactor activated sludge system. *Water Res.*, **50**: 350-358.
- Zia F, Ghafoor N, Iqbal M and Mehboob S. 2016. Green synthesis and characterization of silver nanoparticles using *Cydonia oblong* seed extract. *Appl. Nanosci.*, **6**: 1023-1029.